ORIGINAL ARTICLE

Shiliang Zhang · Danilo D. Fernando

Structural, histochemical, and protein analysis of male reproductive development in willow

Abstract Information on the development of the male reproductive structures in willow will help advance our understanding of its reproductive behavior and contribute to our ability to work towards its improvement. Willow also offers the opportunity to study male sterility, a subject matter which is not typically dealt with in woody plants. As compared to the three willow species examined (*Salix eriocephala*, *S. exigua*, and *S. purpurea*), pollen development in *S. discolor* 'S365' showed several abnormalities starting with the delay in meiosis. This lasted for about 10 days and meiosis eventually occurred as manifested by the formation of microspores. However, most of the resulting microspores collapsed, while only a few developed into pollen grains. The large number of undeveloped and disintegrated microspores appeared to make the few pollen grains sticky, preventing them from being dispersed. Histochemical analysis showed that meiosis in most species of willow was associated with the presence of large amounts of insoluble polysaccharides in the anther wall layers, but only very few of these were observed in *S. discolor*. Also, a 32-kDa protein which is the most abundant protein in the reproductive structures of willow, was absent in *S. discolor* 'S365'. Proteomic analysis showed that this is similar to the storage proteins in *Populus* x *canadensis* and *P. deltoides*. Therefore, male sterility in *S. discolor* may be due to some genetic defects affecting the accumulation of essential reserves in its reproductive structures. The mechanism behind this is unknown, but this study has established the nature of sterility in *S. discolor* 'S365'.

Keywords Male sterility · Pollen abortion · Pollen development · Storage proteins · Willow

S. Zhang · D. D. Fernando
Department of Environmental and Forest Biology,
State University of New York,
College of Environmental Science and Forestry,
241 Illick Hall, 1 Forestry Drive,
Syracuse, NY 13210, USA

Introduction

Willows are fast growing woody plants that are rapidly coming to the forefront as a major source of biomass, an excellent alternative source of energy. It is also a renewable and carbon dioxide neutral energy source. Willow biomass can be used to generate electricity by co-firing it with coal; it can be burned directly or converted to gas or liquid fuel (McIlveen-Wright et al. 2001; Wilson et al. 2001). Various research efforts to increase willow biomass have focused on the requirements of short-rotation plantation culture (Borjesson 1999; Perttu 1999; Aravanopoulos 2000; Nienow et al. 2000; Hunter 2002), interspecific hybridization (Larsson 1998; Kopp et al. 2002; Hallgren et al. 2003), and isolation of molecular markers (Alstrom-Rapaport et al. 1998; Hanley et al. 2002; Barker et al. 2003; Gunter et al. 2003).

Reproductive sterility in plants is a desirable feature because it allows nutrients and assimilates to be redirected to vegetative growth, therefore, contributes to the increase in biomass (Fielding 1960; Ledig and Linzer 1978; Strauss et al. 1995). It was estimated that production of pine cones and pollen grains reduced the stem's mean annual increment by 16% (Fielding 1960). Of the reproductive structures, the anther undergoes the highest rate of metabolism and is therefore the strongest sink in the floral buds (Lawrence and Mayne 1991; Clément et al. 1994, 1996; Clément and Audran 1995; 1999). Therefore, preventing reproductive development may boost growth rates because the energy and nutrients devoted to the formation of reproductive structures are redirected towards vegetative growth (Jain and Minocha 2000; Shykoff et al. 2003).

Our knowledge of male sterility is essentially confined to herbaceous plants such as tobacco (Worrall et al. 1992), tomato (Gorman et al. 1996), maize (Levings 1993; Chaubal et al. 2000), and soybean (Smith et al. 2002) among others. This is mainly because woody plants have long life cycles that make them a difficult

group to work with. However, the use of fast growing hardwoods may be able to offset this problem. Over the years, it has been observed that a few willow clones do not produce pollen grains or seeds (Kopp 2000). In all crosses involving a male clone of *Salix discolor* 'S365', seeds were not obtained (Kopp 2000). It is possible that this clone is reproductively sterile, but it is not known if the observed sterility is a stable genetic condition or simply an environmental effect. If this clone is sterile, the nature of its sterility is not known. Therefore, an opportunity exists that allows exploration of sterility in woody species, a subject matter that is not commonly dealt with in this group of plants. Also, information on the development of the male reproductive structures in willow is lacking. This is important to help advance our understanding of the species' reproductive behavior and facilitate research on this potentially economically valuable species.

This study aims to: (1) determine the timing of the various stages of male reproductive development, (2) describe the development of the male reproductive structures (inflorescence, floral meristem, anther, and pollen grains), (3) identify the onset of pollen grain abortion in *S. discolor* 'S365' by comparing its development with other willow species, (4) characterize pollen development through histochemistry, and (5) identify proteins which are associated with the sterility observed in *S. discolor* 'S365'.

Materials and methods

Plant material

Salix discolor 'S365', *S. eriocephala* 'S19' and '287', *S. exigua* 'S301' and *S. purpurea* 'PUR12' growing at the SUNY-ESF's Genetic Field Station in Tully, NY, USA were the primary species used in this study. Collections and observations were performed from 2001 to 2004. Two types of twigs (of approximately 20-inches long) were collected. Dormant twigs were collected in November and December and stored in a cold room (4°C) until further use. The twigs were induced to produce catkins in a greenhouse and served as source of specimens (inflorescence meristems, anthers, and developing pollen grains) prior to their availability in the field. Some experiments used catkins at various stages produced under field conditions that were collected in April and May. These twigs were used to confirm the developmental stages and structures that were observed using greenhouse-induced catkins.

Ultrastructural analysis

Reproductive buds at inflorescence meristem stage were fixed in 2.5% (w/v) glutaraldehyde in 0.1 M sodium cacodylate buffer (pH 7.4) for 24 h. The samples were rinsed with the same buffer three times for 15 min each and dehydrated by passing them through a graded series of ethanol (50, 70, 95, and 100%) for 15 min each. This was followed by critical point drying, mounting on aluminum stubs, and sputter coating with gold. The samples were examined under a JEOL JSM−5800 LV scanning electron microscope and representative images were obtained.

Histological analysis

Anthers at different developmental stages were collected from both types of twigs at different times of the year. The anthers were fixed for 24 h in 2.5% (v/v) glutaraldehyde in 0.1 M sodium cacodylate buffer (pH 7.4) containing 0.5% (w/v) SDS to reduce the surface tension of specimens. The anthers were rinsed with the same buffer three times for 15 min each. The samples were dehydrated through a graded series of ethanol (50, 70, 95, and 100% ethanol for 15 min each). Infiltration was performed by passing the samples through the following: (1) 1:1 ratio of 100% ethanol to Technovit 7,100 infiltration solution (Heraeus Kulzer, Germany) (composed of 2-hydroxyethyl methacrylate and dibenzoylperoxide) for 4 h; (2) 1:2 ratio of 100% ethanol to infiltration solution for 4 h; (3) pure infiltration solution for about 12 h; and (4) fresh infiltration solution for 24–72 h. The samples were embedded in a medium containing 1:15 ratio of dimethyl sulfoxide to pure infiltration solution. Specimens were allowed to polymerize for 40–120 min at room temperature while completely sealed with paraffin. The specimens were sectioned (1 µm) with a Sorvall MT2-B ultramicrotome using glass knives. The sections were individually picked up and transferred with a fine forcep, floated on a drop of water on glass slides and heated gently to hasten the spreading of the sections. The sections were stained with 0.05% (w/v) Toluidine Blue O (TBO) in 0.2 M sodium phosphate buffer (pH 7) for 30 s and then rinsed with distilled water.

Histochemical analysis

Representative sections were stained with 0.01% (w/v) Aniline Blue in 0.1 M phosphate buffer (pH 9) to detect the presence and localization of callose (Eschrich and Currier 1964). The sections were examined under a LEICA fluorescence microscope using UV excitation (395–415 nm).

Another set of sections representing various developmental stages was stained with Periodic Acid-Schiff's (PAS) to detect the presence and localization of insoluble polysaccharides (Feder and O'Brien 1968). The specimens were examined under a light microscope (Leica DMLB, CA, USA) and representative images were obtained using a DEI-7500 CE digital video camera (Optronics, Goleta, CA, USA).

Protein analysis

Proteins from whole catkins, anthers only, and catkin axes only (anthers removed) were isolated from four clones (three species), i.e., *S. discolor* 'S365', *S. eriocephala* 'S19' and 'S287', *S. exigua* 'S301'. Samples were ground into a fine powder using liquid nitrogen and collected in a sterile microtube. Extraction of proteins was based on Fernando et al. (2001). Briefly, protein extraction buffer composed of 65 mM Tris, 1% sodium dodecyl sulfate, 5% glycerol, and 2.5% β-mercaptoethanol at pH 6.8 was added to the ground specimens and vortexed for 5 min. The solution was boiled for 5 min and then frozen at $-80°C$ for 1 h. Samples were thawed, boiled for 5 min, and centrifuged at $14,000 \times g$ at 4°C for 30 min. The supernatant was collected and stored at $-20°C$ until use. Proteins were quantified using Bio-Rad Protein Assay Kit (Bio-Rad, Hercules, CA, USA). Five dilutions of the bovine serum albumin (BSA) standard and samples were tested by measuring the absorbance at 595 nm. SDS-PAGE was carried out on 1.5-mm thick 12% separating gel and 4% stacking gel. A sample volume of 100 µl containing 50 µg protein was applied in each well. Low range molecular mass standards (14.4–97.4 kDa, Bio-Rad) were used to calibrate the samples. The gel was stained with Coomassie Stain Solution (Bio-Rad).

Two-dimensional SDS polyacrylamide gel electrophoresis was performed according to O'Farrell (1975). Briefly, in the first dimension, isoelectric focusing (IEF) was carried out in glass tubes (2.0-mm inner diameter) with 2% (v/v) ampholine (Gallard-Schlesinger Industries, Inc., Garden City, NY, USA), pH 4–8 for 9,600 volt-h. The tube gel was calibrated by adding 50 ng of tropomyosin to each sample prior to loading. Tropomyosin is an IEF internal standard that showed two polypeptide spots (33 and 34 kDa) of similar pI (5.2). After equilibration in buffer "0" (10% glycerol, 50 mM dithiothreitol, 2.3% SDS and 0.0625 M Tris, pH 6.8), each tube gel was sealed to the top of a stacking gel that overlays a 12% acrylamide slab gel (0.75-mm thick). SDS gel electrophoresis was carried out for about 5 h at 25 mA/gel. High range molecular mass standards (Bio-Rad) were used and appeared on the basic side of the Coomassie blue-stained gels. The gels were dried between transparent cellulose sheets.

Protein spots were excised, washed, reduced with DTT (10 mM in 100 mM NH_4CO_3), alkylated with iodoacetamide (55 mM in 100 mM NH_4CO_3), and rinsed. The proteins were digested in 50 µl 10 mM Tris–HCl (pH 8.0) containing 1 pM trypsin (Sigma, St. Louis, MO, USA) at 37°C for 10–12 h. The peptides were extracted with 25 mM NH_4CO_3, acetonitrile and 5% formic acid. The peptides were purified from the extract using C18 Zip-Tips (Millipore, Bedford, MA, USA) and analyzed by electrospray ionization-quadruple time of flight-tandem mass spectrometry (ESI-QTOF-MS/MS). Fragmentation spectra of each sample were manually analyzed and de novo amino acid sequences were generated. These were submitted for identification using the Mascot interface (Matrix Science, London, UK) and NCBI was selected as the primary database to be searched.

Results

Timing of male reproductive development

The timing of the development of the male reproductive structures in *S. eriocephala* 'S19' and 'S287', *S. exigua* 'S301', *S. purpurea* 'PUR12' and *S. discolor* 'S365' was observed throughout the 4-year duration of this study based on field collected samples (Table 1). Reproductive buds were formed around the middle of July. They were produced at the leaf axils of branches from current year's growth. Compared to vegetative buds, the reproductive buds were usually thicker and bigger. At this stage, reproductive buds were composed of inflorescence meristems with several developing bracts along their flanks (Fig. 1A). Epidermal hairs started to develop on the most distal bracts and progressed towards the bracts at the apical end of the inflorescence meristem. By the middle of August, floral meristems started to develop at the axils of each bract (Fig. 1B). Two anther primordia were formed per floral meristem and no other structure was observed between anther primordia (Fig. 1C). By September, most of the epidermal hairs had formed and completely enclosed the developing inflorescences and the anthers within. At this stage, the anthers were composed of microspore mother cells (MMCs). The reproductive buds remained at this stage throughout the fall and winter.

In April of the following year, pollen development proceeded inside the reproductive buds with the MMCs undergoing meiosis and resulting in the formation of microspore tetrads. The first stage of gamete formation also occurred at this stage. As a result of the growth in the anthers, the reproductive buds started to expand and elongate resulting in the shedding of bud scales. Although the anthers were fully developed, the filaments had not elongated at this stage. In May, the filaments had elongated and resulted in the raising up of the anthers. The

Table 1 Correlation between developmental stages and time of the year in willow

Developmental stage	J	F	M	A	M	J	J	A	S	O	N	D
Reproductive bud	X	X	X				X	X	X	X	X	X
Inflorescence meristem							x	x				
Floral meristem								x				
Anther primordium								x				
Microspore mother cell	x	x	x						x	x	x	x
Tetrad		x										
Microspore		x										
Binucleate pollen grain		x		x								
Flowering/anthesis				X	X							
Anther dehiscence				x	x							

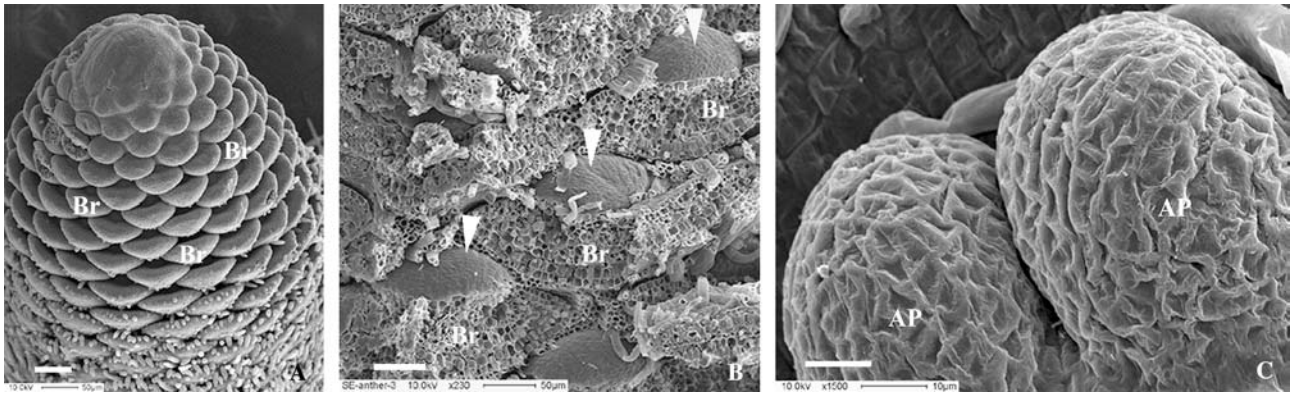X and x = indicate occurrence of developmental stages

Fig. 1 Scanning electron micrographs of male reproductive structure in *Salix discolor*. **A** Inflorescence meristem with developing bracts. *Br* bract. *Bar* = 50 μm. **B** Male floral meristems (*arrow heads*) at the axils of each bract. *Br* bract. *Bar* = 50 μm. **C** Two anther primordia produced per floral meristem. *AP* anther primordium. *Bar* = 10 μm

anthers dehisced at this stage. It was also at this stage when the male flowers were considered in bloom. Of the three species representing four clones examined (*S. eriocephala* 'S19' and 'S287', *S. exigua* 'S301', *S. purpurea* 'PUR12'), no difference was observed in the timing of the various developmental stages (Table 1).

Structural analysis of pollen development

The anthers of *S. eriocephala* 'S19' (Fig. 2A), *S. exigua* 'S301' (data not shown), and *S. discolor* 'S365' (Fig. 2a) were tetrasporangiate. Each lobe was made up of five morphologically distinct groups of cells which included the epidermis, endothecium, middle layer, tapetum, and MMCs (Fig. 2A, a). All of these were made up of a single layer of cells, except for the MMCs, which formed a disorganized mass of cells that occupied the anther locule. At this stage, the tapetum was made up of small cells which were cytologically indistinguishable from the cells of the middle layer (Fig. 2A, a).

In early spring, the MMCs in *S. eriocephala* and *S. exigua* underwent meiosis and formed tetrads of microspores (Fig. 2B). The tetrads were enclosed within a thick callose wall. The tetrads were formed synchronously within an anther lobe but not necessarily between lobes. The tapetal cells became extensively enlarged and well differentiated from the other layers (Fig. 2B).

The microspores became separated from their tetrad arrangement as the callose wall disintegrated. Most of the microspores expanded and assumed an isodiametric shape (Fig. 2C). The tapetal cells remained enlarged, densely cytoplasmic and closely attached to each other (Fig. 2C). At late microspore stage, the tapetal cells became highly vacuolate and separated from one another (Fig. 2D). The anther lobes expanded at this stage. Most of the microspores were densely cytoplasmic, whereas a few appeared collapsed or empty.

Most of the microspores divided to form binucleate pollen grains. These pollen grains were generally densely

cytoplasmic and furnished with intricate wall sculpturing. At this stage, the tapetal cells had almost completely degenerated (Fig. 2E). The cells of the endothecium became expanded and acquired secondary wall thickenings. As the anthers dehisce (Fig. 2F), numerous pollen grains were released with sizes ranging from 20 μm to 36 μm.

A comparison of pollen development between *S. eriocephala*, *S. exigua*, and *S. discolor* revealed several interesting peculiarities in the latter. One of the striking differences was the delay of meiosis in *S. discolor*. Based on the typical developmental stages represented in *S. eriocephala* 'S19' and 'S287' and *S. exigua* 'S301', meiosis occurred when the tapetal cells were fully expanded and densely cytoplasmic. In *S. discolor*, meiosis did not take place even if the tapetal cells were in this condition. Instead, the MMCs became enlarged and separated from one another (Fig. 2b). Also, correlated with the occurrence of meiosis was callose wall formation. In *S. eriocephala*, meiosis and callose wall formation occurred simultaneously resulting in the retention of the four haploid microspores in tetrad arrangement. In *S. discolor*, even if the MMCs did not undergo meiosis (Fig. 2b), formation of callose wall still occurred (Fig. 3a).

▶

Fig. 2A–F Photomicrographs of anther and pollen development in *S. eriocephala* 'S19'. **A** MMC stage and each anther lobe is made up of epidermis, endothecium, middle layer, tapetum, and microspore mother cells. **B** Tetrad stage with distinct and enlarged tapetum, callose walls surround the microspores. **C** Early microspore stage showing the microspores (*arrow heads*) separated from each other. **D** Late microspore stage showing the degenerating tapetum. **E** Binucleate pollen grain stage and the tapetal cells almost completely disintegrated. **F** Anther dehiscence. **a–f**. Photomicrographs of anther and pollen development in *S. discolor* 'S365'. **a** MMC stage and each anther lobe is made up of epidermis, endothecium, middle layer, tapetum and microspore mother cells. **b** Enlarged MMC showing enlarged tapetum and formation of callose wall. **c** Early microspore stage showing many collapsed microspores (*arrow heads*), the tapetum is still enlarged. **d** Late microspore stage showing degenerating tapetum. **e** Binucleate pollen grain stage and the tapetum has almost completely degenerated. **f** Anther dehiscence showing few normal appearing pollen grains *CW* callose wall, *EM* enlarged microspore mother cells, *Ep* epidermis, *En* endothecium, *ML* middle layer, *MMC* microspore mother cell, *Ta* tapetum, *Te* tetrad. *Bars* = 40 μm

After about 10 days, microspores were formed in *S. discolor* (Fig. 2c). Apparently, meiosis occurred but it was never observed. The tapetum at this stage was still made up of enlarged and densely cytoplasmic cells. The callose wall was dissolved and the microspores were released from their tetrad arrangement (Fig. 2c). However, most of the released microspores were collapsed.

At late microspore stage, the tapetum became highly vacuolate and separated from each other (Fig. 2d). This stage of development was accompanied by increase in the diameter of the anther lobes.

In *S. discolor*, a few microspores underwent mitosis resulting in the formation of binucleate pollen grains. The tapetum had almost completely degenerated at this
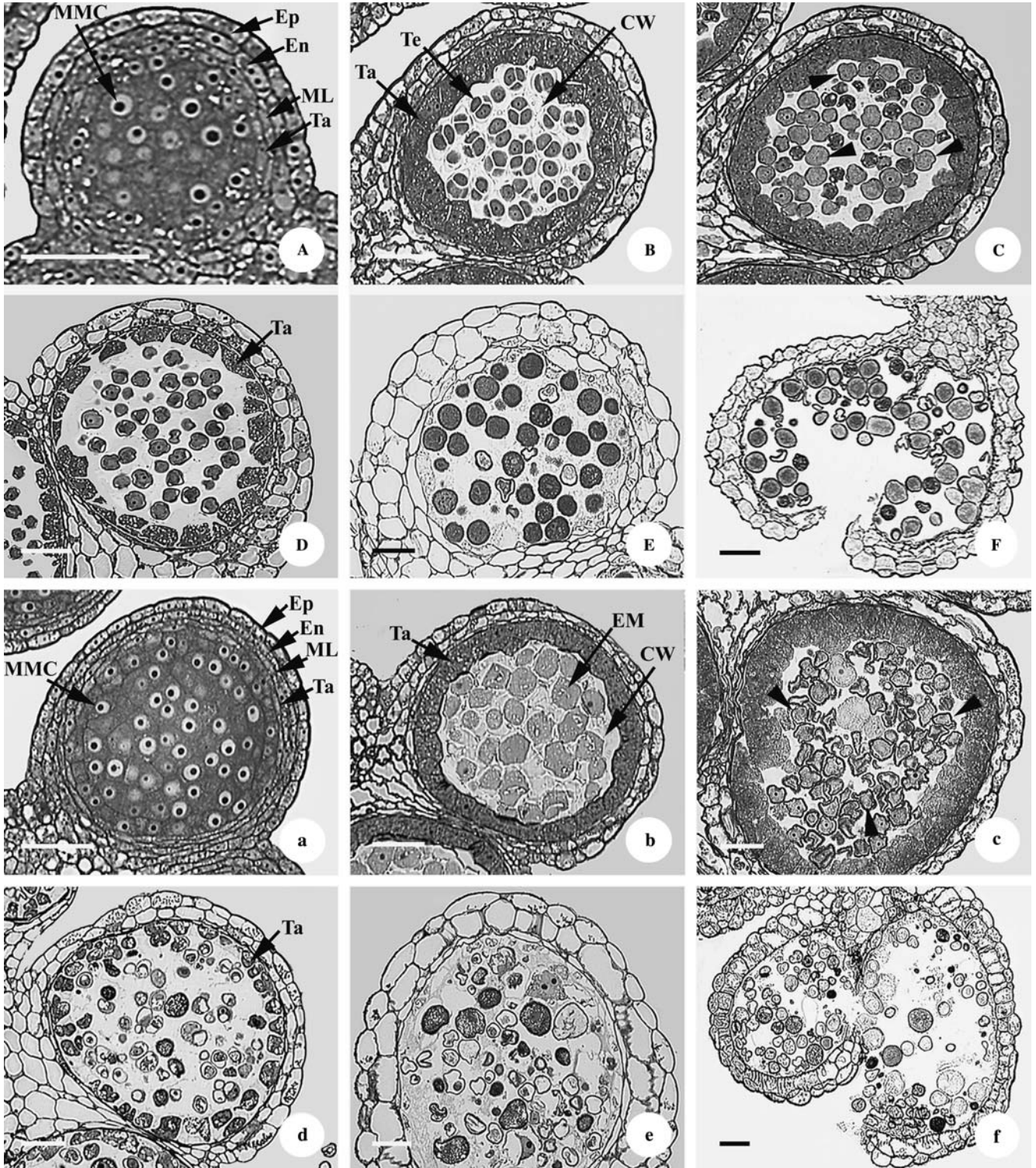
stage (Fig. 2e). The anthers dehisced but the pollen grains remained attached on the inner part of the anther wall (Fig. 2f).

Histochemical analysis of pollen development

Anthers at various stages of development were examined for the presence and localization of callose using aniline blue. Callose appeared bright blue or white when observed under a fluorescence microscope using UV excitation. At MMC stage, no callose was detected from any of these species. In *S. eriocephala* and *S. exigua*, callose was observed only at the tetrad stage (Fig. 3A). In *S. discolor*, callose was observed in the undivided but separated MMCs (Fig. 3a) at the stage where the tapetal cells were fully expanded and the cytoplasm ranged from being cytoplasmically dense to slightly vacuolate.

To detect the presence and localization of insoluble polysaccharides in anthers at various developmental stages, representative sections were stained with Periodic-Acid-Schiff's (PAS). Structures that were PAS-positive stained red. In *S. eriocephala* and *S. exigua*, a few PAS-positive granules were observed in the anther wall layers and connective tissues at MMC stage. Accumulation of large amounts of PAS-positive granules in the anther wall layers and connective tissues occurred during meiosis and tetrad formation (Fig. 3B). No PAS-positive granules were observed in the MMCs, tetrads and enlarged tapetal cells at this stage. At microspore stage, the number of PAS-positive granules in the anther

wall layers and connective tissues decreased. PAS-positive granules had completely disappeared at the pollen grain stage and no PAS-positive granules were observed in the anther wall layers.

In *S. discolor*, there were far fewer PAS-positive granules in the anther wall layers and connective tissues at MMC stage. At the stage where meiosis and tetrad formation were expected to occur based on the developmental and cytological features of the tapetum, also very few PAS-positive granules were observed in the anther wall layers and connective tissues in *S. discolor* (Fig. 3b).

Protein analysis

Proteins were extracted from whole reproductive buds, inflorescence axes, and anthers of *S. eriocephala* 'S19' and 'S287' and *S. discolor* 'S365' and separated by 1D gel electrophoresis (Fig. 4). Our results showed that in both clones of *S. eriocephala*, the most abundant protein in all the reproductive structures examined was a 32-kDa protein. In *S. discolor*, this protein is largely absent in all the reproductive structures examined. Protein profiles from the reproductive buds and stems of *S. exigua* and *S. purpurea*, as well as stems of *S. eriocephala* and *S. discolor*, were also examined and showed the presence and abundance of the 32-kDa protein (data not shown).

Analysis by 2D gel electrophoresis showed that the 32-kDa protein was made up of six isoforms with the following isoelectric points (p*I*): 6.3, 6.5, 6.8, 7.4, 8.1 and

Fig. 3 A–B. Histochemical analysis of pollen development in *S. eriocephala* 'S19'. **A** Callose walls (*white*) at tetrad stage. **B** Periodic Acid Schiff (*PAS*)-positive granules (*arrow heads*) in anther wall and connective tissue. **a–b** Histochemical analysis of pollen development in *S. discolor* 'S365'. **a** Callose walls (*white*) in the enlarged MMC. **b** Few of PAS-positive granules (*arrow head*) in the anther walls. *Bars* = 40 μm
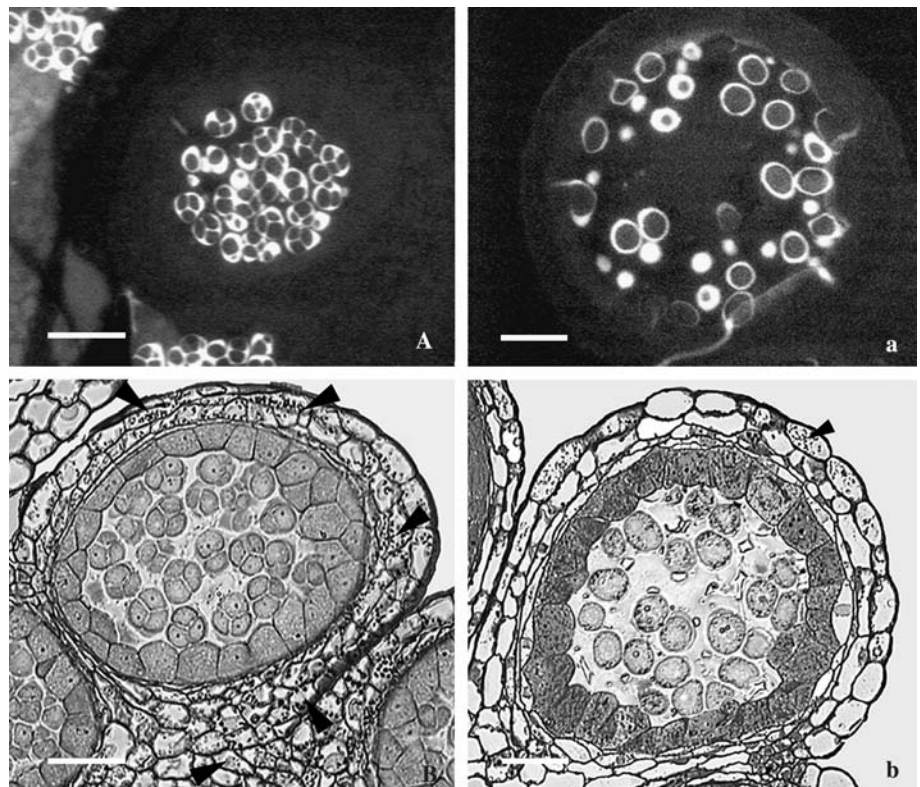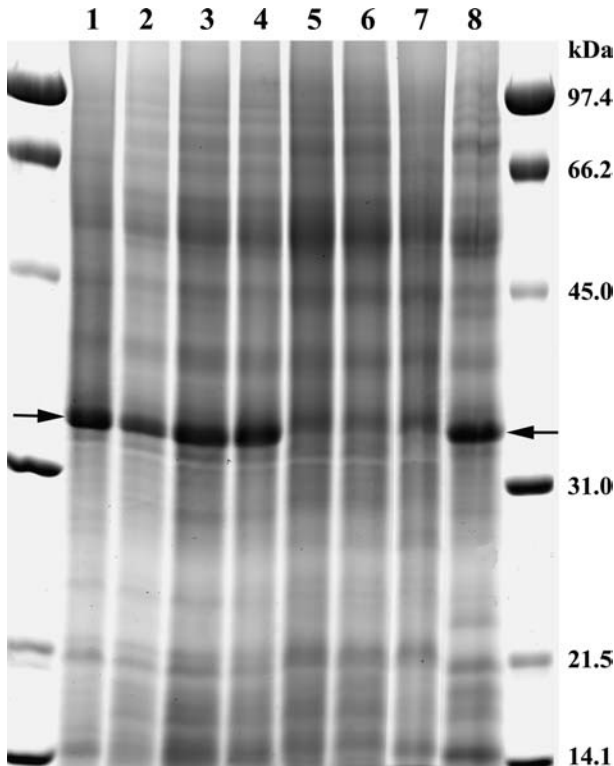
Fig. 4 One-dimensional polyacrylamide gel analysis of proteins from reproductive structures in *S. eriocephala* 'S19'and 'S287' and *S. discolor* 'S365'. Lane 1 catkin axis 'S287'; Lane 2 whole catkin 'S287'; Lane 3 whole catkin without hairs 'S287'; Lane 4 anther 'S287'; Lane 5 anther 'S365'; Lane 6 whole catkin 'S365'; Lane 7 catkin axis 'S365'; Lane 8 whole catkin 'S19'. The *arrows point* to the 32-kDa protein

8.6 (Fig. 5). The two most intense spots (p*I* 6.8 and 7.4) were subjected to ESI-QTOF-MS/MS analysis followed by manual interpretation of the spectra. De novo sequencing yielded information on the amino acid sequences from several peptides. The amino acid sequences obtained from the two spots were identical. Although analysis by mass spectrometry could detect posttranslational modifications, no such information was obtained from the two spots examined. However, the amino acid sequences obtained (Table 2) were queried against the NCBI's non-redundant protein database using BLAST. Sequences from the positive hits were aligned for comparison with the sequences from *S. eriocephala* (Table 2).
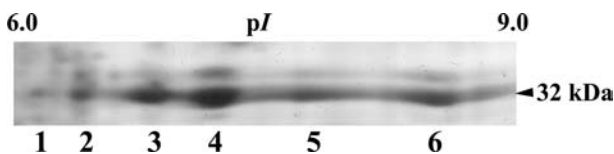

Fig. 5 2D SDS polyacrylamide gel analysis of the 32-kDa protein from *S. eriocephala*. 1 p*I* = 6.3; 2 p*I* = 6.5; 3 p*I* = 6.8; 4 p*I* = 7.4; 5 p*I* = 8.1; 6 p*I* = 8.6

Discussion

Development of male reproductive structures in willow

Reproductive buds in willows were formed by the middle of July and contained developing inflorescence meristems. Floral meristems were initiated acropetally along its flanks. By the middle of August, two anther primordia were initiated per floral meristem. It is at this stage when the gender of the plant can first be determined. Dissection of the reproductive buds and examining developing anthers allow determination of the male plants. This is about 8 months earlier as compared to waiting for the appearance of the anthers in spring. The ability to determine male plants early in development will be useful in the planning and execution of experiments, thereby facilitating breeding work. Our dissection technique is equally applicable to the determination of female plants and very useful for the identification of gender from plants that have produced reproductive buds. However, if gender determination is desired from younger plants, molecular markers should be used (Alstrom-Rapaport et al. 1998; Gunter et al. 2003).

By September, the anthers were at microspore mother cell stage and it was in this condition that the plant underwent winter dormancy. This stage is comparable to many other woody species that produced reproductive buds that overwinter (Pacini et al. 1986; Luna et al. 1990; Reinoso et al. 2002). Much of the activities in the reproductive buds in the first year of the reproductive process were in the stages leading to the initiation of the anthers (containing microspore mother cells). As for the second year of the reproductive process, the activities lead to the actual development of the pollen grains.

Our histological analysis shows that there is no difference in the development of the reproductive structures, particularly of the pollen grains between the two clones of *S. eriocephala* 'S19' and 'S287' that were examined (results for 'S287' not shown). Except for the timing, there is also no difference in the development of pollen grains between those induced under greenhouse conditions and those obtained directly from the field. Furthermore, no difference was observed in the development of pollen grains between *S. eriocephala* and *S. exigua* or *S. purpurea*. Therefore, based on these comparisons, the series of developmental stages documented in *S. eriocephala* represent a typical condition in willow, from which stages in other willow species could be compared with. *S. eriocephala* was used as the standard since *S. discolor* with normal stages of pollen development was not available during the study.

The nature of male sterility in *S. discolor* 'S365'

There are several differences in the development of the pollen grains in *S. discolor* when compared to what we

Table 2 Partial amino acid sequence of the 32-kDa protein from *S. eriocephala* and comparison with other proteins in the NCBI database

Species (accession#)	Amino acid sequence and alignment
S. eriocephala (?)	NGLVLTSDEVEK??VVFQGVSNVAGETLK ?????Y LASYNAFLAATK ?
P. x canadensis (AAB20113.2)	ASVALTSLSNEKLFVVFQGVSNVAGETSS NSRVS YLASYNAFLAATK 299
P. deltoides (Q07469)	ASVALTSLSNEKLFVVFQGVSNVAGETSS NSRVS YLASYNAFLAATK 299
P. deltoides (Q09117)	ASVALTSLSNEKLFVVFQGVSNVAGETSS NSRVS YLASYNAFLAATK 316

? = not known available

consider as typical for willows. In *S. eriocephala* and *S. exigua*, meiosis occurs as the tapetum fully enlarges. In *S. discolor*, however, meiosis does not occur even if the tapetum is at this developmental condition. Instead, the microspore mother cells expand and separate from each other. These were never observed in the microspore mother cells of *S. eriocephala* and *S. exigua*.

Also, correlated with the occurrence of meiosis in *S. eriocephala* and *S. exigua* is callose wall formation which results in the retention of the microspore tetrads within the callose wall. In *S. discolor*, formation of callose wall occurs in spite of the absence of meiosis or microspores suggesting that callose wall formation is unaffected by the developmental condition of the developing male gametophytes. Therefore, callose walls enclose the enlarged microspore mother cells in *S. discolor*. In spite of this, meiosis still occurs in *S. discolor*, although after about 10 days. On the other hand, most of the resulting microspores from *S. discolor* are unable to expand and they eventually disintegrate. The remaining few microspores expand and undergo microspore mitosis. The large number of degenerated microspores appears to form a sticky coating around the few bicellular pollen grains which are not easily dispersed when the anthers dehisce. When these pollen grains were extracted using organic solvents and used to pollinate various willow clones, seeds were not produced (Kopp 2000). This indicates that even the few normal appearing pollen grains that are produced by *S. discolor* are non-functional.

Another difference between the two willow species is in the degree of accumulation of insoluble carbohydrates in the anther wall layers surrounding the microspore mother cells. A lot of insoluble carbohydrates were observed in *S. eriocephala*, much fewer in *S. discolor*. This is related to what was observed in *Brassica juncea* where sugar levels in the anther of male sterile lines were found to be significantly lower than in those of the related fertile lines (Banga et al. 1984). Also, deficiency of carbohydrates in anthers has been reported to lead to abnormal pollen development and male sterility (Banga et al. 1984; Bhadula and Sawhney 1989; Sawhney 1992). Carbohydrates are known to serve as energy source to sustain the active metabolism associated with pollen development (Clément et al. 1994). Reproductive organs are potentially sensitive to modification of carbohydrate supply, particularly at meiosis (Saini 1997; Jean and Lapointe 2001). Therefore, the limited amount of insoluble polysaccharides in the anther wall layers and connective tissues of *S. discolor* might have deprived the microspore mother cells, thereby retarding their development.

Analysis of the protein profiles of the inflorescence meristem, inflorescence axis, and anthers of *S. eriocephala* by 1D gel electrophoresis shows that the most abundant protein in these structures is a 32-kDa protein. This protein was also found in the stems of *S. eriocephala* and *S. discolor*, as well as in the other willow clones and species examined. However, this protein is highly reduced in the inflorescence meristem, inflorescence axis and anthers of *S. discolor*. A 32-kDa protein was also described in *S. microstachya* (Wetzel and Greenwood 1991), poplars (Clausen and Apel 1991; Coleman et al. 1992; Coleman and Chen 1993; Bearmore et al. 1996), and pistachio (Golan-Goldhirsh et al. 1998). Identification of the 32-kDa protein by 2D gel electrophoresis coupled with ESI-Q-TOF-MS/MS analysis using sequences from several peptides showed that it is highly homologous to the major storage proteins in *Populus × canadensis* (Clausen and Apel 1991) and bark storage protein in *P. deltoides* (Coleman et al. 1992; Coleman and Chen 1993). No other homolog proteins were obtained through BLAST search. In fact, this protein may be a characteristic of the Salicaceae (Beardmore et al. 1996).

Storage proteins are translocated in perennial tissues in the fall and remobilized to serve as source of carbon, nitrogen and sulfur for growth and development in spring (Herman and Larkins 1999). The anther is the strongest sink in the floral buds, and intense anther growth occurs from microspore mother cell stage to late microspore stage (Clément et al. 1994; 1996). This means that the delay in the activity of the microspore mother cells (i.e., meiosis) may also be attributed to the much reduced amount of the major storage protein in the reproductive buds of *S. discolor*.

The series of developmental defects associated in the formation of pollen grains in *S. discolor* is typically observed in plants with perturbed carbohydrate and protein accumulations (Goetz et al. 2001; Datta et al. 2002). This suggests that male sterility in *S. discolor* 'S365' is due to some genetic defects that affect the accumulation of carbohydrate and protein reserves in the reproductive structures. The exact mechanism behind these deficiencies and their effect on pollen development in willow is not known. However, it is significant to be able to establish the nature of male sterility in *S. discolor* 'S365'.

Male sterility is a highly desirable feature and various researches have been done to achieve this by disrupting pollen development through genetic engineering (Strauss et al. 1995; Goetz et al. 2001; Daniell 2002; Guerineau et al. 2003). It is remarkable that male sterile plants are available even without resorting to genetic engineering, especially in species with a very high economic potential like willow.

References

Alstrom-Rapaport C, Lascoux M, Wang YC, Roberts G, Tuskan GA (1998) Identification of a RAPD marker linked to sex determination in the basket willow (*Salix viminalis* L.). J Hered 89:44–49

Aravanopoulos FA (2000) Absence of association between heterozygosity and biomass production in *Salix exigua* Nutt. Theor Appl Genet 100:1203–1208

Banga SS, Laban KS, Banga SK (1984) Male sterility in Indiana mustard (*Brassica juncea* (L.) Coss.) – a biochemical characterization. Theor Appl Genet 67:515–519

Barker JHA, Pahlich A, Trybush S, Edwards KJ, Karp A (2003) Microsatellite markers for diverse *Salix* species. Mol Ecol Notes 3:4–6

Beardmore T, Wetzel S, Burgess D, Charest P J (1996) Characterization of seed storage proteins in *Populus* and their homology with *Populus* vegetative storage proteins. Tree Physiol 16: 833–840

Bhadula SK, Sawhney VK (1989) Amylolytic activity and carbohydrate levels during the stamen ontogeny of a male fertile and a "gibberellin-sensitive" male sterile mutant tomato (*Lycopersicon esculentum*). J Exp Bot 40:789–794

Borjesson P (1999) Environmental effects of energy crop cultivation in Sweden-I: identification and quantification. Biomass Bioenergy 16:137–154

Chaubal R, Zanella C, Trimnell MR, Fox TW, Albertsen MC, Bedinger P (2000) Two male-sterile mutants of *Zea mays* (Poaceae) with an extra cell division in the anther wall. Am J Bot 87:1193–1201

Clausen S, Apel K (1991) Seasonal changes in the concentration of the major storage protein and its mRNA in xylem ray cells of poplar trees. Plant Mol biol 17:669–678

Clément C, Audran JC (1995) Anther wall layers control pollen sugar nutrition in *Lilium*. Protoplasma 187:172–181

Clément C, Audran JC (1999) In: Clément C, Pacini E, Audran JC (eds) Anther and Pollen. From biology to biotechnology. Springer, Heidelberg Berlin Newyork, pp 69–90

Clément C, Chavant L, Burrus M, Audran JC (1994) Anther starch variations in *Lilium* during pollen development. Sex Plant Reprod 7:347–356

Clément C, Burrus M, Audran JC (1996) Floral organ growth and carbohydrate content during pollen development in *Lilium*. Am J Bot 83:459–469

Coleman GD, Chen THH (1993) Sequence of a poplar bark storage protein gene. Plant Physiol 102:1347–3–1348

Coleman GD, Chen THH, Fuchigami L (1992) cDNA cloning of poplar bark storage protein and control of its expression by photoperiod. Plant Physiol 98:687–693

Daniell H (2002) Molecular strategies for gene containment in transgenic crops. Nat Biotechnol 20:581–586

Datta R, Chamusco KC, Chourey PS (2002) Starch biosynthesis during pollen maturation is associated with altered patterns of gene expression in maize. Plant Physiol 130:1645–1656

Eschrich W, Currier HB (1964) Identification of callose by its diachrome and fluorochrome reactions. Stain Technol 39:303–307

Feder N, O'Brien TP (1968) Plant microtechnique; some principles and new methods. Am J Bot 55:123–142

Fernando DD, Owens JN, Yu X, Ekramoddoullah AKM (2001) RNA and protein synthesis during in vitro pollen germination and tube elongation in *Pinus monticola* and other conifers. Sex Plant Reprod 13:259–264

Fielding JM (1960) Branching and flowering characteristics of Monterey pine. Forestry and timber bureau bulletin 37. Commonwealth Government Printer, Canberra, Australia

Goetz M, Godt DE, Guivarch A, Kahmann U, Chriqui D, Roitsch T (2001) Induction of male sterility in plants by metabolic engineering of the carbohydrate supply. Proc Natl Acad Sci USA 98:6522–6527

Golan-Goldhirsh A, Peri I, Birk Y (1998) Inflorescence bud proteins of *Pistacia vera*. Trees 12:415–419

Gorman SW, Banasiak D, Fairley C, Cormick S (1996) A 610 kb YAC clone harbors 7 cM of tomato (*Lycopersicon esculentum*) DNA that includes the *male sterile 14* gene and a hotspot for recombination. Mol Gen Genet 251:52–59

Guerineau F, Sorensen A, Fenby N, Scott RJ (2003) Temperature sensitive diphtheria toxin confers conditional male-sterility in *Arabidopsis thaliana*. Plant Biotechnol J 1:33–42

Gunter L E, Roberts G T, Lee K, Larimer W, Tuskan A (2003) The development of two flanking SCAR markers linked to a sex determination locus in *Salix viminalis* L. J Hered 94:185–189

Hallgren P, Ikonen A, Hjalten J, Roininen H (2003) Inheritance patterns of phenolics in F1, F2, and back-cross hybrids of willows: implications for herbivore responses to hybrid plants. J Chem Ecol 29:1143–1158

Hanley S, Barker JHA, Van Ooijen JW, Aldam C, Harris SL, Ahman I, Larsson S, Karp A (2002) A genetic linkage map of willow (*Salix viminalis*) based on AFLP and microsatellite markers. Theor Appl Genet 105:1087–1096

Herman E, Larkins B (1999) Protein storage bodies and vacuoles. Plant Cell 11:601–613

Hunter T, Peacock L, Hunter H, Brain P (2002) Effect of plantation design on stem-infesting form of rust in willow biomass coppice. For Pathol 32:87–97

Jain SM, Minocha SC (2000) Molecular biology of woody plant. Vol. I. Kluwer Scientific Publisher, Dordrecht, The Netherlands, pp 135–153

Jean D, Lapointe L (2001) Limited carbohydrate availability as a potential cause of fruit abortion in *Rubus chamaemorus*. Physiol Plant 112:379–387

Kopp RF (2000) Genetic improvement of *Salix* using traditional breeding and AFLP fingerpring. PhD Dissertation. State University of New York College of Environmental Science and Forestry, Syracuse, NY.

Kopp RF, Smart LB, Maynard AC, Tuskan TA, Abrahamson LP (2002) Predicting within-family variability in juvenile height growth of *Salix* based upon similarity among parental AFLP fingerprints. Theor Appl Genet 105:106–112

Larsson S (1998) Genetic improvement of willow for short rotation coppice. Biomass Bioenergy 15:23–26

Lawrence DK, Mayne RG (1991) Plant growth regulators and photosynthesis. In: Baker NR, Percival MP (eds) Herbicides. Elsevier Science, New York, pp 299–335

Ledig FT, Linzer DIH (1978) Fuel crop breeding. Chemtech 8:18–27

Levings CS III (1993) Thoughts on cytoplasmic male sterility in *cms-T* maize. Plant Cell 5:1285–1290

Luna V, Lorenzo E, Reinoso H, Tordable MC, Abdala G, Pharis RP, Bottini R (1990) Dormancy in peach (*Prunus persica* L.) flower buds. I. Floral morphogenesis and endogenous gibberellins at the end of the dormancy period. Plant Physiol 93:20–25

McIlveen-Wright DR, Williams BC, McMullan JT (2001) A reappraisal of wood-fired combustion. Bioresour Technol 76:183–190

Nienow S, McNamara KT, Gillespie AR (2000) Assessing plantation biomass for co-firing with coal in northern Indiana: a linear programming approach. Biomass Bioenergy 18:25–135

O'Farrell PH (1975) High resolution two-dimensional electrophoresis of proteins. J Biol Chem 250:4007–4021

Pacini E, Bellani LM, Lozzi R (1986) Pollen, tapetum and anther development in two cultivars of sweet cherry (*Prunus avium*). Phytomorphotogy 36:197–210

Perttu KL (1999) Environmental and hygienic aspects of willow coppice in Sweden. Biomass Bioenergy 16:291–297

Reinoso H, Luna V, Pharis RP, Bottini R (2002) Dormancy in peach (*Prunus persica*) flower buds. V. Anatomy of bud development in relation to phonological stage. Can J Bot 80:656–663

Saini HS (1997) Effects of water stress on male gametophyte development in plants. Sex Plant Reprod 10:67–73

Sawhney VK (1992) Floral mutants in tomato: development, physiology, and evolutionary implications. Can J Bot 70:707–710

Shykoff J, Kolokotronis SO, Collin C, López-Villavicencio (2003) Effects of male sterility on reproductive traits in gynodioecious plants: a meta-analysis. Oecologia 135:1–9

Smith MB, Palmer RG, Horner HT (2002) Microscopy of a cytoplasmic male-sterile soybean from an interspecific cross between *Glycine max* and *G. soja* (*leguminosae*). Am J Bot 89:417–426

Strauss SH, Rottmann WH, Brunner AM, Sheppard LA (1995) Genetic engineering of reproductive sterility in forest trees. Mol Breeding 1:5–26

Wetzel S, Greenwood JS (1991) The 32-kilodalton vegetative storage protein of *Salix microstachya turz*. Plant Physiol 97:771–777

Wilson E, Chapman PJ, McDonld A (2001) Merging nitrogen management and renewable energy needs. Sci World J 22:1 Suppl 2:745–749

Worrall D, Hird DL, Hodge R, Paul W, Draper J, Scott R (1992) Premature dissolution of the microsporocyte callose wall causes male sterility in transgenic tobacco. Plant Cell 4:759–771